

Optical trapping of gold aerosols

Regina K Schmitt^a, Liselotte Jauffred^{a,b}, S. Mohammad-Reza Taheri^c, Heiner Linke^a and Lene B. Oddershede^b

^aNanoLund and Solid State Physics, Lund University, Box 118, 22100 Lund, Sweden;

^bThe Niels Bohr Institute, University of Copenhagen, Blegdamsvej 17, 2100 Copenhagen, Denmark;

^cPhysics Department, Institute for Advanced Studies in Basic Sciences (IASBS), P. O. Box 45195-1159, Zanjan, Iran

ABSTRACT

Aerosol trapping has proven challenging and was only recently demonstrated.¹ This was accomplished by utilizing an air chamber designed to have a minimum of turbulence and a laser beam with a minimum of aberration. Individual gold nano-particles with diameters between 80 nm and 200 nm were trapped in air using a 1064 nm laser. The positions visited by the trapped gold nano-particle were quantified using a quadrant photo diode placed in the back focal plane. The time traces were analyzed and the trapping stiffness characterizing gold aerosol trapping determined and compared to aerosol trapping of nanometer sized silica and polystyrene particles. Based on our analysis, we concluded that gold nano-particles trap more strongly in air than similarly sized polystyrene and silica particles. We found that, in a certain power range, the trapping strength of polystyrene particles is linearly decreasing with increasing laser power.

Keywords: Aerosol, air, optical tweezers, gold nano-particles, polystyrene nano-particles, power spectral analysis, laser manipulation, power spectral analysis, aerotaxy

1. INTRODUCTION

In 1975, for the first time, Ashkin and Dziedzic used the radiation pressure of light to balance gravitation and balance airborne glycerol droplets.² In 1997 Omori et al.³ reported optical trapping (as opposed to levitation) of a dielectric particle in air using a single tightly focused laser beam. In air, dielectric particles⁴ and liquid droplets have been optically trapped^{5,6} and even multiple droplets have been trapped by holographic optical tweezers.⁷ Not just the translation, but also the rotation of microparticles in air, has been proven recently.⁸ In liquid, the first optical control of individual metal nano-particles (NP) by Svoboda et al,⁹ showed that due to their larger inducible polarizability, gold NPs trap even more readily than polystyrene particles of similar size. Since then, while the optical trapping range of gold- and silver-NPs has been significantly expanded,¹⁰⁻¹² essentially no progress has been reported on optical trapping of metallic NPs in air or vacuum. This may be related to practical challenges which include faster Brownian motion of aerosols because of the lower viscosity, reduced heat dissipation, and larger optical aberration in comparison to trapping in water. Spherical aberration, arising due to refractive index mismatch between chamber, water and air has been predicted by Mie Debye spherical aberration theory (MDSA) to make the trapping of small particles in air difficult.¹³ The ability to manipulate and study individual metal or semiconductor nanostructures in air or vacuum would open up many exciting opportunities.^{14,15} For example, optical trapping of individual gold particles could enable *in situ* studies of the nucleation and growth processes active in Aerotaxy.¹⁶

Here, we summarize results recently published¹ where we demonstrated optical trapping of individual airborne gold NPs with diameters from 80 nm to 200 nm and compared to aerosol trapping of similarly sized di-electric particles. We performed a quantitative analysis of the positions visited by the trapped particles and calculate the spring constants characterizing optical trapping of metallic NPs in air. Additionally, we discuss the spring constant as a function of applied power and asymmetries of the lateral component of the trapping strength.

Further author information:

Lene Oddershede: E-mail: oddershede@nbi.dk

Heiner Linke: E-mail: heiner.linke@ftf.lth.se.

2. METHODS

2.1 Experimental set-up

The experimental set-up is based on an infrared laser beam ($\lambda = 1064$ nm, Nd:YVO4, Spectra Physics BL106C) implemented in an inverted microscope (Leica, DMIRBE) as described earlier.^{17,18} The laser beam is focused into the air chamber, expanded to slightly overfill the back aperture of an immersion oil objective (NA = 1.4, 100 \times , Leica). To minimize spherical aberration we used an immersion media with a refractive index of 1.57 (Cargille) as suggested by Reihani et al¹⁹ and recently investigated for aerosol trapping.²⁰ To minimize turbulence we constructed an air chamber as suggested by Taheri et al,⁴ it consisted of three sub-chambers, compare Figure 1 in [1]. We deliver the NP aerosol with a nebulizer into the upper chamber. One hole between each two subchambers (1 mm diameter) allows a small fraction, assisted by gravitation, to pass to the lowest, least turbulent chamber, the trapping chamber. This final chamber is higher than the maximal working distance of the objective.

The droplets delivered by the nebulizer contain a solution with a particle concentration of 0.1-1 nM, details in.¹ The solution consisted of a mixture of (96 %) ethanol and particle solution, containing gold NPs (80 nm, 150 nm, and 200 nm), PEG coated gold NPs (Nanopartz: 80nm and 150 nm), silica spheres (Bangs Laboratories: 1.010 μ m; Polysciences: 690 nm and 540 nm), and polystyrene beads (Bangs Laboratories: 200 nm, 580 nm, and 960 nm), respectively.

Due to the high dilution of particles in the solution and droplet diameters of circa 5 μ m (visual estimate), only every 50th to 200th droplet carried a particle. As soon as a particle entered the trap (once every ~ 20 minutes at constant aerosol flow) we stopped the flow to ensure only single droplet and, thus, single bead trapping. We trapped gold, polystyrene and silica NPs stably in air for several minutes. We never observed stable trapping of an ethanol droplet as it evaporated instantaneously after trapping.

2.2 Trapping strength

Using the quadrant photodiode, we measured the thermal fluctuations of the NP in the optical trap. In accordance with common practise from trapping particles in liquids²¹ and new results from trapping micron-particles in air,⁸ we assume that the positions measured in Volts by the photodiode, x_V , are proportional to the metric displacement of the particle in the trap, x_m : $x_m = \beta x_V$, with the conversion factor β .

The dynamics of a trapped particle in one translational direction (x) is well described by the Langevin equation:

$$\mathcal{F}(T, t) = \gamma \dot{x} + \kappa x + m \ddot{x}, \quad (1)$$

where m is the mass and $\mathcal{F}(T, t)$ are the stochastic forces that depend on time, t , and temperature, T . The first term, $\gamma \dot{x}$, describes the viscous force with the friction coefficient γ . The second term, κx , describes the force exerted on the particle by the optical trap upon an excursion, x , from the equilibrium position and characterises the strength of the trap. The inertial term, $m \ddot{x}$, can safely be neglected in Eq. 1 when trapping in water, because the movement is overdamped. It is not a priori clear whether this is also valid for trapping in air. If assuming an overdamped situation, Fourier transformation of the overdamped Langevin yields the single-sided positional power spectrum (PSD):

$$S_{\text{PSD}}(f) = \beta^2 \frac{k_B T}{2\gamma\pi^2(f_c^2 + f^2)}, \quad (2)$$

where k_B is the Boltzmann factor and the corner frequency, f_c , is the ratio between the trap stiffness, κ , and the friction coefficient, γ . A typical powerspectrum from a trapped gold NP in air is shown in Figure 3b, and as apparent from this figure, a simple Lorentzian function (Eq. 2) fits quite well to data from a metallic NP trapped in air. The power spectral analysis directly returns f_c and hence κ , as well as the conversion factor β . The calibration method outlined above assumes that the dynamics of the trapped particle is overdamped. We have shown that the gold NPs trapped in air can be considered overdamped¹ as can be expected for an estimated Reynolds number of 10^7 . All results for spring constants shown were normalized with laser power at the sample plane. An air condenser placed over the chamber was used to collect the back-scattered light and image it onto a quadrant photo diode (QPD, S5981, Hamamatsu) placed in the back focal plane. The acquisition frequencies were 22 kHz for the dielectric particles and 50 kHz for the gold NPs for denser sampling at high frequencies.

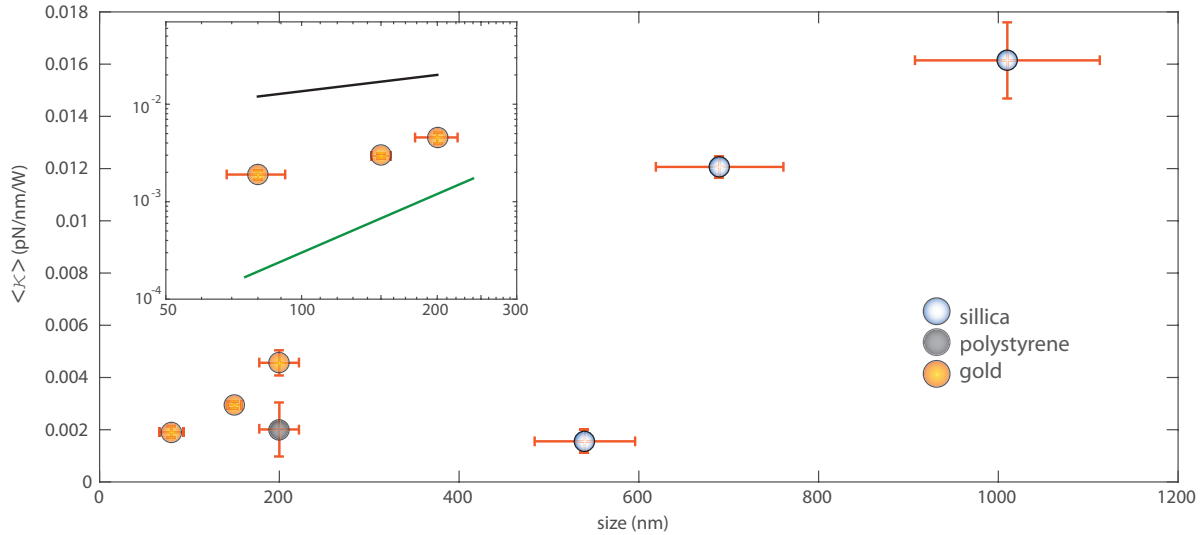


Figure 1. Trapping strength $\langle \kappa \rangle$ (normalized with laser power) increases with particle size. Gold NPs (yellow) trap more strongly than similar sized polystyrene particles (grey) and the much larger silica particles (blue). Each value of $\langle \kappa \rangle$ shown is the mean value from at least 5 independent experiments and the error bars show one standard deviation. The error bars on particle diameter are as given by the manufacturer. The inset shows a double logarithmic plot of $\langle \kappa \rangle$ versus diameter for the gold NPs. The green line has a slope of 2 and the black line shows the scaling of κ for gold NPs of similar size in water.¹⁰ Reproduced with permission from Nano Letters.¹

3. RESULTS

It follows the analysis of the trapping strength, κ , for silica, polystyrene and gold particles in dependence of the particle size and for polystyrene in dependence of the laser power. We found that, for gold and polystyrene NPs, the strength of the optical trap increases with particle size,¹ Figure 1. Furthermore for similarly sized particles, gold NPs trapped more strongly than polystyrene NPs, and also stronger than the much larger (450 nm) silica NPs.¹ The trapping strength of gold NPs in air was thereby circa $1/10^1$ of the trapping strengths obtained for gold NPs^{10,12} or other spherical NPs^{11,22,23} in water.

For a quantitative analysis of the relation between trapping strength and particle size, Rayleigh optics can be used, because the particles investigated here are much smaller than the wavelength of the laser (1064 nm). The particle is then considered as a dipole in an electromagnetic field under the influence of the scattering force F_{sc} , the absorption force F_{abs} and the gradient force F_{grad} . F_{grad} is proportional to the polarizability, α , which is proportional to the polarizable volume, V . For small particles, this volume can be identified with the particle volume. For particles with radii larger than the skin depth of gold, $\delta = 23 \text{ nm}$ ⁹ at 1064 nm, the volume needs to be adjusted, because the field intensity decays exponentially inside the particle. The polarizable volume is instead V' ⁹:

$$V' = 4\pi \int_0^R r^2 \exp\left(\frac{r-R}{\delta}\right) dx, \quad (3)$$

where R is the radius of the particle. This correction results in the scaling: $F_{grad} \propto R^2$. For this reason, one would expect κ , from particles with radii larger than the skin depth, to scale as R^2 . However, the plot of $\langle \kappa \rangle$ versus diameter on double logarithmic axes in the inset of Figure 1 clearly shows that the scaling is smaller than quadratic (the green line has a slope of 2). We suppose that spherical aberrations are the reason for this scaling that is similar to the scaling observed in water¹⁰ (shown by a black line in the inset). In accordance with this conception, Hajizadeh et al could reach a scaling corresponding to 3 in water only when spherical aberration was significantly reduced.¹² For dielectric spheres with diameters from 200 nm to $1 \mu\text{m}$ $\langle \kappa \rangle$ is expected to increase with d until it reaches the lateral extent of the focus ($\sim 1 \mu\text{m}$).²⁴ This is also observed in Figure 1 for the silica particles. In accordance with the early results of trapping gold versus dielectric NPs in liquid⁹ we found that also in air, gold NPs have larger κ than similarly sized dielectric particles.¹

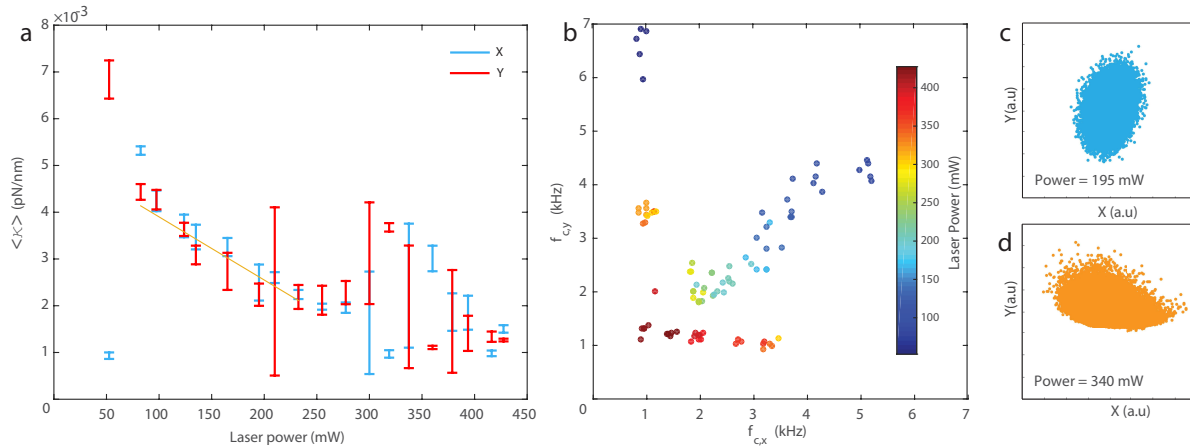


Figure 2. Asymmetric and symmetric trapping of a 960 nm polystyrene bead for Laser powers between 50 mW and 430 mW at the sample plane. a) For power values between 100 mW and 260 mW, the trap stiffness, $\langle \kappa \rangle$, in the two lateral directions x (blue) and y (red) is in good agreement and, in this power regime, there is a linear response between and laser power. However, $\langle \kappa \rangle$ is decreasing with power in contradiction to what is expected for optical trapping in water. Excerpt was published in Nano Letters;¹ Reproduced with permission from Nano Letters. b) For very low and very large power trapping becomes asymmetric. Displayed is the characteristic frequency f_c in x and y direction for various Laser powers. c)& d) Typical positions explored by a trapped polystyrene particle. At intermediate powers (195 mW) the pattern is rather symmetrical, whereas for high powers (340 mW) a strong asymmetry is apparent.

Because it was easier to stably trap airborne polystyrene particles, also at relatively low laser powers, than trapping airborne gold NPs, we performed a systematic study of how the spring constant, κ , characterizing aerosol polystyrene particle trapping in the lateral directions varied with laser power. The laser power at the sample plane was varied from 50 mW to 430 mW and κ as a function of laser power is shown in Figure 2. For laser powers between 100 and 260 mW, $\langle \kappa \rangle$ is linearly dependent on power.¹ Interestingly, it shows opposite behaviour to the trapping behaviour of gold and polystyrene particles in water: $\langle \kappa \rangle$ decreases with increasing laser power. In axial direction Mie Debye Spherical Aberration Theory (MDSA) predicts indeed a decrease of κ in a certain power regime¹³ for aerosol trapping due to the shift of the trapping position away from the focus in axial direction that is caused by the increased laser power. This shift can be expected to lead to a decrease of F_{grad} not only in axial direction¹³ but also in lateral direction. For large and very low laser powers the trap becomes asymmetric, which is especially apparent if displaying the characteristic frequencies, f_c , in the lateral x and y direction as has been done in Figure 2b. Figure 2c shows the typical positions explored by a particle that was trapped at the intermediate power of 195 mW. Space in both lateral directions is explored rather evenly. For a bead trapped at a higher power of 340 mW, the particle shows strong confinement in y-direction and lower confinement in x-direction. We suppose that the asymmetry is caused by spherical aberration. MDSA indicates a strong effect of aberrations on the trap properties.¹³ We can assume to have high aberration, because we are using an objective that is optimized for focussing visible light in water, not for focusing 1064 nm light in air. However, even in water, the focus of an infrared laser beam has been found to be severely aberrated and gold NPs trapped in water in such an aberrated focus have been observed to remain stably trapped in lobes with relatively low intensity, in particular the larger particles were prone to off-maximum trapping.¹⁸ This is further supported by a study of semiconducting NPs (quantum dots) which only rarely ($< 5\%$ of the time) are trapped in the highest intensity region.²⁵ Therefore supposedly the beads are trapped in asymmetric side lobe at high and low Laser powers. The overall sensitivity of the trapping properties on Laser power might be a reason why aerosol trapping has been so challenging.

One of the major concerns of this study was to ensure that only single particles were trapped. Therefore we diluted the particle solution to a very low concentration of particles (on average 1 particle per ~ 100 droplets). Because the droplet size was small ($\approx 5 \mu\text{m}$) it is unlikely that more than one particle is carried by each droplet. This is true as long as the particles have not agglomerated before the droplets are formed. To minimize agglomeration in the stock solution we did experiments with PEG coated particles. After the droplets enter the trap, the

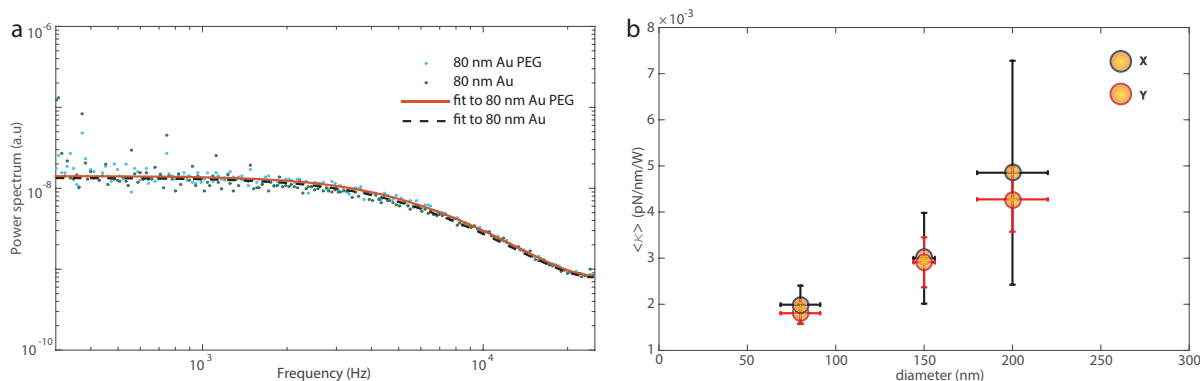


Figure 3. a) Power spectra of the positions visited by two 80 nm gold particles, one with PEG coating (light blue dots) and without any coating (green dots). The lines denote Lorentzian fits (of Eq. 2 using the program from Ref.²⁶) to the data from the PEG coated particle (full red line, $f_c = 5290 \pm 132$ Hz) and from the uncoated particle (dashed black line, $f_c = 5185 \pm 120$ Hz), respectively. The two data sets and their fits overlap and return corner frequencies, f_c , which are indistinguishable within the error bars. b) The average spring constant, κ , for trapping airborne gold NPs are indistinguishable within the error bars (one standard deviation) in the two lateral directions. The two orthogonal directions are x (black circles) and y (red circles), where x is along the laser polarization, are indistinguishable within the error bars. Figures reproduced with permission from Nano Letters.¹

temperature of both the ethanol droplet and the captured gold NP increases due to absorption. Temperatures above the boiling point of ethanol (351° K) are reached immediately, leading to a complete evaporation of the ethanol droplet (and possibly the PEG coating) within microseconds. Indeed, we observed in brightfield imaging that the particles are delivered to the trap in a liquid droplet that evaporates immediately leaving a single gold NP trapped. Our experiments were performed on a time scale much larger than the evaporation (seconds); all results shown are from a situation where ethanol has evaporated. Comparing the results for PEG coated gold NPs and non-coated gold NPs revealed no difference,¹ Figure 3a. The data in Figure 1 is from both types of experiments. Furthermore, the trapping characteristics of the two lateral directions were similar,¹ Figure 3b. If the metallic NPs had been elongated (for example because a small number of particles stick together), and not spherical, they would have aligned along the laser polarization (which is one of the lateral directions measured) and a difference in the two orthogonal lateral directions would have been observed.²⁷ As the spring constants, characterizing the two lateral directions, within the error bars are identical, it is quite likely that the investigated metallic NPs were spherical as expected.

Furthermore, for all experiments with gold NPs, the error bars of κ are rather small. We conclude that it is very likely that we most often trap only a single particle at a time.

In accordance with what is presented here, we want to point out that our set-up with the deliverable method as described has the advantage as opposed to other set-ups, that no liquid layer is formed on top of the cover slide. This layer would introduce an additional diffraction index mismatch, leading to increased spherical aberration and worse trapping characteristics.¹³ Varying thickness of the liquid layer would lead to varying focal points, trap positions and trapping strength.¹³ Therefore, even though we can not prevent aberrations completely, this method guarantees the same aberrations for all experiments. For a trap that is symmetric and with the relation between κ and power being equal every time, single particle trapping is reasonably ensured. We emphasize that both the reduction of turbulence and spherical aberrations, and the single particle trapping that are achieved with the chamber design and deliverable method are key-points for our successful trapping experiments.

4. DISCUSSION

All the spherical gold NP sizes investigated here, with diameters from 80 nm to 200 nm, could be optically trapped in air, stably and individually. It is likely that also aerosol particles beyond this size interval and with different composition and shapes can be stably trapped and future efforts will explore the limits. In comparison to similarly sized silica or polystyrene particles, gold NPs trap more strongly in air, however, with spring constants

that are approximately ten times smaller than for trapping similar particles in water. For polystyrene NPs, in a certain power regime, the trapping strength decreases linearly with the applied laser power. For very low and very high powers, the lateral components of the trapping strength appear asymmetrical, possibly caused by trapping in side loops due to spherical aberration. Both phenomena, the negative linear dependence and the asymmetry of the trapping strength, should be further explored (also for metal NPs) in order to fully understand their origin. Another effect that is more prominent in air than in water is heating due to the lower heat conductance of air. We discuss the heating of airborne gold NPs in Ref [1]. Generally, modelling and mapping of the aberrated intensity distribution and exact knowledge of the trapping positions will likely improve aerosol trapping techniques. Hopefully, future efforts will address these topics and utilize the presented techniques to construct, investigate and control metallic nanostructures in air, away from the surfaces.

ACKNOWLEDGMENTS

The author acknowledge fruitful discussions and advice from J. Johansson, S. N. S. Reihani, and P. M. Bendix and financial support from the Excellence Program at the University of Copenhagen and from the Knut and Alice Wallenberg Foundation at NanoLund, Lund University (nmC@LU).

REFERENCES

- [1] Jauffred, L., Taheri, S. M.-R., Schmitt, R., Linke, H., and Oddershede, L. B., “Optical Trapping of Gold Nanoparticles in Air,” *Nano Letters* **15**, 4713–4719 (2015).
- [2] Ashkin, A. and Dziedzic, J. M., “Optical Levitation of Liquid Drops by Radiation Pressure,” *Science* **187**, 1073–1075 (1975).
- [3] Omori, R., Kobayashi, T., and Suzuki, A., “Observation of a single-beam gradient-force optical trap for dielectric particles in air,” *Optics Lett.* **22**(11), 816 (1997).
- [4] Taheri, S. M. R., Sadeghi, M., Madadi, E., and Reihani, S. N. S., “Tube length-assisted optimized aerosol trapping,” *Opt. Commun.* **329**, 196–199 (2014).
- [5] Magome, N., Kohira, M. I., Hayata, E., Mukai, S., and Yoshikawa, K., “Optical Trapping of a Growing Water Droplet in Air,” *J. Phys. Chem. B* **107**(16), 3988–3990 (2003).
- [6] Hopkins, R. J., Mitchem, L., Ward, A. D., and Reid, J. P., “Control and characterisation of a single aerosol droplet in a single-beam gradient-force optical trap,” *Phys. Chem. Chem. Phys.* **6**(21), 4924–4927 (2004).
- [7] Burnham, D. R. and McGloin, D., “Holographic optical trapping of aerosol droplets,” *Opt. Express* **14**(9), 4175–4181 (2006).
- [8] Arita, Y., Mazilu, M., and Dholakia, K., “Laser-induced rotation and cooling of a trapped microgyroscope in vacuum,” *Nature Commun.* **4**, 2374 (2013).
- [9] Svoboda, K. and Block, S. M., “Optical trapping of metallic Rayleigh particles,” *Opt. Lett.* **19**(13), 930–932 (1994).
- [10] Hansen, P. M., Bhatia, V. K., Harrit, N., and Oddershede, L. B., “Expanding the optical trapping range of gold nanoparticles,” *Nano Lett.* **5**(10), 1937–1942 (2005).
- [11] Bosanac, L., Aabo, T., Bendix, P. M., and Oddershede, L. B., “Efficient optical trapping and visualization of silver nanoparticles,” *Nano Lett.* **8**(5), 1486–1491 (2008).
- [12] Hajizadeh, F. and Reihani, S. N. S., “Optimized optical trapping of gold nanoparticles,” *Opt. Express* **18**(2), 551–559 (2010).
- [13] Burnham, D. R. and McGloin, D., “Modelling of optical traps for aerosols,” *Journal of the Optical Society of America B* **28**(12), 2856–2864 (2010).
- [14] Yue, W., Wang, Z., Yang, Y., Chen, L., Syed, A., Wong, K., and Wang, X., “Electron-beam lithography of gold nanostructures for surface-enhanced Raman scattering,” *J Micromech. Microeng.* **22**(12), 125007 (2012).
- [15] Mendes, P. M., Jacke, S., Critchley, K., Plaza, J., Chen, Y., Nikitin, K., Palmer, R. E., Preece, J. a., Evans, S. D., and Fitzmaurice, D., “Gold nanoparticle patterning of silicon wafers using chemical e-beam lithography,” *Langmuir* **20**(9), 3766–3768 (2004).

- [16] Heurlin, M., Magnusson, M. H., Lindgren, D., Ek, M., Wallenberg, L. R., Deppert, K., and Samuelson, L., "Continuous gas-phase synthesis of nanowires with tunable properties," *Nature* **492**(7427), 90–4 (2012).
- [17] Richardson, A., Reihani, S. N. S., and Oddershede, L. B., "Combining confocal microscopy with precise force-scope optical tweezers," *Proc. SPIE* **6326**, 6326 (2006).
- [18] Kyrsting, A., Bendix, P. M., and Oddershede, L. B., "Mapping 3D focal intensity exposes the stable trapping positions of single nanoparticles," *Nano Letters* **13**(1), 31–35 (2013).
- [19] Reihani, S. N. S. and Oddershede, L. B., "Optimizing immersion media refractive index improves optical trapping by compensating spherical aberrations," *Opt. Lett.* **32**(14), 1998–2000 (2007).
- [20] Taheri, S. M. R., Madadi, E., Sadeghi, M., and Reihani, S. N. S., "Optimized three-dimensional trapping of aerosols: the effect of immersion medium," *Journal of the Optical Society of America B* **32**, 1494–1498 (2015).
- [21] Ott, D., Reihani, S. N. S., and Oddershede, L. B., "Crosstalk elimination in the detection of dual-beam optical tweezers by spatial filtering," *Review of Scientific Instruments* **85**, 053108 (2014).
- [22] Jauffred, L. and Oddershede, L. B., "Two-photon quantum dot excitation during optical trapping," *Nano Lett.* **10**(5), 1927–1930 (2010).
- [23] Jauffred, L., Richardson, A. C., and Oddershede, L. B., "Three-dimensional optical control of individual quantum dots," *Nano Lett.* **8**(10), 3376–3380 (2008).
- [24] Rohrbach, A., "Stiffness of Optical Traps: Quantitative Agreement between Experiment and Electromagnetic Theory," *Phys. Rev. Lett.* **95**(16), 168102 (2005).
- [25] Jauffred, L., Kyrsting, A., Arnspang, E. C., Reihani, S. N. S., and Oddershede, L. B., "Sub-diffraction positioning of a two-photon excited and optically trapped quantum dot," *Nanoscale* **6**(12), 6997–7003 (2014).
- [26] Hansen, P. M., Tolić-Nørrelykke, I. M., Flyvbjerg, H., and Berg-Sørensen, K., "tweezercalib 2.0: Faster version of MatLab package for precise calibration of optical tweezers," *Comp. Phys. Commun.* **174**(6), 518–520 (2006).
- [27] Selhuber-Unkel, C., Zins, I., Schubert, O., Sönnichsen, C., and Oddershede, L. B., "Quantitative optical trapping of single gold nanorods," *Nano Letters* **8**(9), 2998–3003 (2008).